Sound scattering by a lattice of resonant inclusions in a soft medium

Alex Skvortsov* and Ian MacGillivray
Defence Science and Technology, 506 Lorimer Street, Fishermans Bend, Victoria 3207, Australia

Gyani Shankar Sharma and Nicole Kessissoglou
School of Mechanical and Manufacturing Engineering, University of New South Wales, Sydney, New South Wales 2052, Australia

(Received 11 April 2019; published 28 June 2019)

We present a generalized analytical model to investigate acoustic scattering by a lattice of voids of arbitrary shape in a viscoelastic matrix. To this end, we represent the lattice of voids using effective boundary conditions that incorporate multiple scattering effects. Applying analogies between acoustics and electrostatics, the model is derived for voids of nonspherical shape and different lattice arrangements. Our analytical results are compared with those from numerical simulations as well as experimental results from the literature.

DOI: 10.1103/PhysRevE.99.063006

I. INTRODUCTION

The interaction of elastic waves with arrays of resonant scatterers has traditionally been a focus of research in acoustics and materials science (for example, see Refs. [1–9] and references therein). These studies have provided insightful understanding of new wave phenomena such as wave trapping and localization, nonlinear wave interaction, subwavelength focusing, and cloaking, which are important for many practical applications including nondestructive defect detection [10,11], acoustic tomography [12], and biomedical diagnostics [13,14]. In particular, soft media embedded with a periodic arrangement of inclusions, often referred to as phononic crystals, have become a favorable candidate for noise control applications, for example, as anechoic coatings on marine vessels. Effective conversion of longitudinal to shear waves arises from subwavelength resonance of the inclusions, resulting in strong attenuation of sound [15–22]. This effect is a direct result of the softness of the material or, more specifically, the relatively small shear wave speed compared with the speed of longitudinal waves in the material. The threshold conditions for the softness of a voided soft elastic medium in order for subwavelength resonance to occur are described in Ref. [22]. The shape of inclusions (spheres, cylinders, or disks), their material properties (voids, elastic, or hard scatterers), filling fraction of the inclusions, and their configuration in the material play an important role in acoustic performance [16,17,23–27].

Multiple scattering effects in locally resonant phononic crystals are also important for sound attenuation depending on the concentration of scatterers, their distribution, and the frequency of the incident acoustic wave [28]. One seminal study by Foldy [29] examined propagation of acoustic waves in a medium with a random distribution of point monopole inclusions. The effective wave number of the acoustic wave propagation was derived in terms of the scattering amplitude of an individual inclusion and filling fraction of the scatterers. The results are valid for a relatively low concentration of inclusions and at frequencies low enough such that the acoustic wavelength is greater than the mean distance between the scatterers [28]. Importantly, the analytical approach pioneered by Foldy [29] is valid for frequencies above subwavelength resonance in a soft elastic material and as such allows for treatment of acoustic metamaterials with strong resonant properties using effective medium theory even in the limit of relatively high volume fraction.

For a regular distribution of resonant scatterers embedded in a soft elastic medium, multiple scattering effects have been shown to lead to exotic phenomena, one of which is superabsorption [16,17,20]. This phenomenon is due to strong coupling between scatterers, which leads to coherent reradiation of waves over ranges less than an acoustic wavelength. To explain this phenomenon, simple analytical models have been developed [20,30,31]. The simplest model has been formulated as scattering of plane acoustic waves at normal incidence by a periodic array of air bubbles in a two-dimensional (2D) square lattice [20]. A single void of radius a subject to an acoustic plane wave of unity amplitude of the form $p_i = e^{(-ikx+i\omega t)}$ generates a scattered spherical wave field given by

$$p_s = (f_{0,s}/r)e^{(-ikr+i\omega t)}, \tag{1}$$

where ω is the angular frequency, $k = \omega/c_l$ is the longitudinal wave number, c_l is the longitudinal wave speed in the host elastic medium, and $i = \sqrt{-1}$. The scattering function $f_{0,s}$ is given by [20,31,32]

$$f_{0,s} = \frac{a}{(\omega_0/\omega)^2 - 1 + i(\delta + ka)}, \tag{2}$$

where ω_0 is the monopole resonance frequency of an individual void when not in a lattice and ka represents the radiation damping. For a single void in an elastic medium of infinite extent, ka is very small. Further, as the subsequent derivations are performed in the long-wavelength regime whereby $ka \ll 1$, we have excluded the radiation damping for simplicity. In a

*alex.skvortsov@dst.defence.gov.au

soft matrix, δ is dominated by viscous losses within the elastic medium and is given by $\delta = 4\eta/\rho a^2\omega$, where ρ is the density and η is the dynamic viscosity of the medium [20]. For a material with complex shear modulus $\mu = \mu' + i\mu''$, the dynamic viscosity is given by μ''/ω, and the resonance frequency and damping are given by the following well-known expressions [33–36]:

$$\omega_0^2 = \frac{4\mu' + 3B'}{\rho a^2}, \tag{3}$$

$$\delta = \frac{4\mu'' + 3B''}{\rho a^2 \omega^2}, \tag{4}$$

where $B = B' + iB''$ is the bulk modulus of air. The limit $\mu \ll (3/4)B$ is the bubble approximation, while $\mu \gg (3/4)B$ corresponds to an evacuated cavity in a soft material [20,36]. The resonance frequency of a single void given by Eq. (3) can also be expressed using $\omega_0 = 2c_t/a$, where $c_t = \sqrt{\mu'/\rho}$ is related to the shear wave speed. The model of a spherical cavity in a soft medium has an intrinsic analogy with sound scattering by a bubble in a liquid, for which ω_0 is then often referred to as the Minnaert frequency [20,37,38].

The reflection coefficient from a sparse array of voided inclusions has been previously derived in terms of the scattering coefficient of an individual void [28]. To account for multiple scattering effects, the total incident pressure on an individual void within a lattice needs to be modified to include the scattered pressure from all other inclusions located within the array. By approximately evaluating the lattice sum for an infinite array of inclusions, the following expression for the reflection coefficient can be derived [30,31,39]:

$$r = \frac{-iKa}{(\omega_0/\omega)^2 - I + i(\delta + Ka)}, \tag{5}$$

where $K = 2\pi/kd^2$, $I = 1 - Ka\sin(\alpha kd)$, and d is the lattice constant (spacing between void centers). The value of the constant α in Ref. [30] is given as $\alpha = 1$ and later refined in Ref. [31] as $\alpha = 1/\sqrt{\pi}$.

Equation (5) predicts a minimum transmission value at a frequency which can be associated with the monopole resonance of the periodic array of voids given by

$$\Omega = \frac{\omega_0}{\sqrt{I}}, \tag{6}$$

where

$$I = 1 - 2\sqrt{\pi}(a/d). \tag{7}$$

Parameter I describes the change in the monopole resonance frequency of a single void, ω_0, to its value within a periodic array of voids, Ω, due to acoustic coupling between the voids arising from multiple scattering effects. Parameter I has also been derived as $I = 1 - 2(a/d)$ [39]. Equations (5) and (6) are valid only when the longitudinal wavelength is greater than the spacing between the scatterers ($kd \ll 1$) and for small filling fraction ($a/d < 0.2$) [40]. Hence, Eq. (5) cannot be used near the full-blockage limit ($a \to d/2$).

In this work, a generalized expression for the reflection coefficient given by Eq. (5), which is valid for a lattice of voids of arbitrary shape, is analytically derived using analogies between acoustics, electrostatics, and diffusion kinetics. The generalized version of Eq. (5) is then incorporated into the conventional transfer matrix method and applied to different 2D lattice configurations for which multiple scattering effects are dominant. Our analytical results are compared with numerical simulations from a finite element model and available experimental data from the literature.

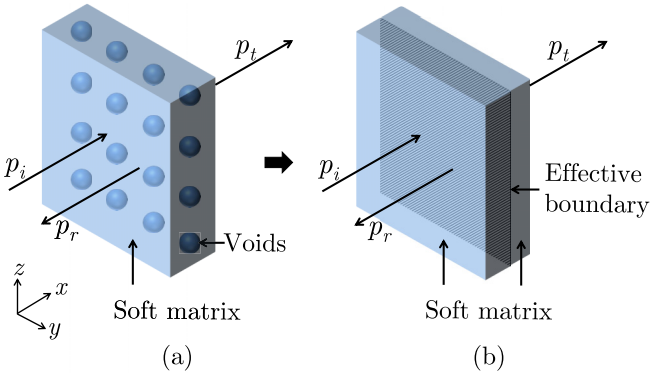

FIG. 1. Schematic diagram showing (a) a lattice of spherical cavities in a host soft elastic medium and (b) the spherical cavities approximated as an effective boundary.

II. MODEL

A. Transfer matrix method

A layer of voids in a viscoelastic medium as shown in Fig. 1(a) is herein approximated as an effective boundary embedded in the host elastic medium [Fig. 1(b)]. The effective boundary is represented as a planar layer of negligible thickness. p_i, p_r, and p_t denote the incident, reflected, and transmitted pressures, respectively. For a lumped planar layer of negligible thickness, continuity of pressure (shown later as appropriate for our void layer) gives the relation $t = 1 + r$, where $t = p_t/p_i$ and $r = p_r/p_i$ are transmission and reflection coefficients, respectively. Using the standard transfer matrix method [41,42], sound propagation through the layer in terms of the total acoustic pressure p and particle velocity v on either side of the interface is given by

$$\begin{bmatrix} p_1 \\ v_1 \end{bmatrix} = \begin{bmatrix} 1 & 0 \\ \chi & 1 \end{bmatrix} \begin{bmatrix} p_2 \\ v_2 \end{bmatrix}, \tag{8}$$

where the subscripts 1 and 2, respectively, refer to the elastic medium on the incidence and transmission sides of the planar layer,

$$\chi = \frac{-2r}{(1+r)Z}, \tag{9}$$

and $Z = \rho c_l$ is the acoustic impedance of the host elastic medium. For specific values of the void radius a, lattice spacing d, and monopole resonance ω_0, Eqs. (5), (8), and (9) form a one-dimensional model of acoustic wave interaction with a plane lattice of void scatterers.

B. Effective scattering function

For voids of nonspherical shape, we apply the electrostatic analogy initially reported by Strasberg [43] and extended in Refs. [28,44,45]. According to this analogy, the added mass

of a nonspherical bubble can be related to the electrostatic capacitance of an ideal conductor with the same shape as the bubble. Specifically, if the permittivity of free space is set to unity, then $C_{0,\mathrm{sph}} = 4\pi a$ is the capacitance of a single sphere of radius a in open space. The effective scattering function of the void within the lattice can be related to the change in capacitance of a single sphere in open space to its capacitance value when altered in shape and placed in a lattice. In the bubble approximation limit of $\mu \ll (3/4)B$, the resonance frequency given by Eq. (3) scales as $\omega_0^2 \propto C_{0,\mathrm{void}}$ [44]. This scaling relation enables a simple derivation of the resonance frequency of a void of different shape but same volume as a sphere. By writing Eq. (2) in terms of void capacitance and normalizing the resulting expression to equivalent sphere values, the effective scattering function for a void within a lattice becomes

$$f_s = \frac{a}{(\omega_0/\omega)^2 - I + i\delta}. \tag{10}$$

Here ω_0 and δ are still given by Eqs. (3) and (4) for a void of equivalent volume to a sphere, and $I = C_{0,\mathrm{sph}}/C = 4\pi a/C$. Parameter I in Eq. (10) will be subsequently shown to be equivalent to the same parameter in Eq. (5). Note that Eq. (10) assumes dominance of the monopole scattering by the voids over other scattering modes, which may be violated for high filling fraction of voids.

C. Effective reflection coefficient

An alternative derivation of the reflection coefficient as in Eq. (5) is presented by employing the method of effective boundary conditions described in Refs. [46–48]. Consider the normal incidence of a plane acoustic wave on a regular planar lattice of monopole scatterers. Due to periodicity of the model, only a unit cell of the system needs to be considered. This allows reduction of the original problem to sound scattering by a monopole scatterer located at the center of a duct with rigid walls of cross-sectional area S, matching the unit cell of the lattice. The duct is oriented along the x axis corresponding to the direction of sound propagation, with the monopole scatterer located at $x = 0$. If the lattice is square, then the duct has width equal to the lattice spacing d, with cross-sectional area $S = d^2$. The frequency ω is assumed low ($kd \ll 1$) such that only the fundamental mode of the waveguide can propagate. Hence, higher-order modes are neglected, although the effect of higher-order responses of the scatterer can be found in Ref. [49].

In the far field of the scatterer ($x \gg a$), but within an acoustic wavelength ($|kx| \ll 1$), the acoustic field can be considered one-dimensional. The effective boundary conditions at $x = 0$ entail continuity of pressure $p(x)$ as well as a discontinuity in particle velocity $v(x)$ on the surface of the planar layer given by $v(0_+) - v(0_-) = V/S$, where V is the volume velocity of the monopole scatterer induced by the acoustic pressure $p(0)$ at $x = 0$. An expression relating the volume velocity to the scattering amplitude and the acoustic pressure at the effective boundary is given by [45]

$$V = \frac{-i4\pi f_s}{\rho\omega} p(0), \tag{11}$$

where the effect of multiple scattering of waves between voids is taken into account using the scattering amplitude given by Eq. (10). Since the gradient of the pressure is related to particle velocity using

$$\frac{\partial p}{\partial x} = -i\rho\omega v, \tag{12}$$

the boundary condition at $x = 0$ can be written in terms of a length parameter l as

$$\frac{p(0)}{l} \equiv i\rho\omega(v(0_+) - v(0_-)) = \frac{i\rho\omega V}{S}. \tag{13}$$

Substituting Eq. (11) into Eq. (13) it follows that

$$l = \frac{S}{4\pi f_s}. \tag{14}$$

Parameter l is also referred to as the blockage length [48]. As the sign of l depends on the assumed time harmonic dependency, it has been set to keep its real part positive at low frequencies. Its frequency dependence arises through f_s given by Eq. (10). Parameter l is generally also dependent on geometry such as scatterer shape, lattice spacing, and lattice morphology.

The effective reflection coefficient can now be described in terms of the length parameter using the transfer matrix given by Eq. (8) relating the pressures and velocities on either side of the effective boundary at $x = 0$ as

$$-\chi = \frac{v(0_+) - v(0_-)}{p(0)} = \frac{2r}{(1+r)Z}. \tag{15}$$

Therefore, from Eqs. (13) and (15),

$$r = \frac{1}{2ikl - 1}. \tag{16}$$

Substituting Eqs. (10) and (14) into Eq. (16), the expression for the reflection coefficient becomes

$$r = \frac{-iKa}{(\omega_0/\omega)^2 - I + i(\delta + Ka)}, \tag{17}$$

where $K = 2\pi/kS$. Equation (17) is identical in form to Eq. (5) whereby K is equivalent to that in Eq. (5) when the lattice is square. Equations (8), (9), and (17) now constitute the transfer matrix framework to study the interaction of acoustic waves with a plane lattice of voids of arbitrary shape.

The method of an effective boundary condition holds for the long-wavelength regime where $ka \ll 1$. For soft materials at resonance, $ka \sim c_t/c_l$ which is equivalent to $\omega/\omega_0 \sim c_l/c_t$. Since for soft materials $c_l/c_t \gg 1$, the equations derived here are also valid at frequencies much higher than resonance.

D. Effect of lattice type and scatterer shape

We herein derive parameter I for voids of arbitrary shape and for different lattice arrangements using an analogy between capacitance and trapping rate of diffusive particles of an absorber of the same shape [50]. Parameter I is first derived for the case of spherical voids within a square lattice, that is, $I_{\mathrm{sph}} = C_{0,\mathrm{sph}}/C_{\mathrm{sph}}$ (noting that the capacitance of a sphere in a lattice, C_{sph}, is different from the same sphere in free space, $C_{0,\mathrm{sph}}$). We begin with the analytical solution for the trapping rate of a lattice of absorbing disks placed on a reflective

TABLE I. Parameter values [51].

Lattice type	q_1	q_2
Triangle	1.62	1.36
Square	1.75	2.02
Hexagonal	1.37	2.59
Random	0.34	−0.58

plane. Due to symmetry arguments, the trapping rate (and hence capacitance) of disks on a reflective plane is half of that of the same lattice of disks in free space [51,52]. To apply this analytical solution for our setting of a lattice of spheres, we use scaling relations to replace the original spheres with equivalent disks. However, a straightforward replacement of a sphere with a disk of the same capacitance violates the preservation of volume underlying Eqs. (10) and (17) and as such needs to be carefully evaluated. To this end, we propose a two-stage replacement. First, we replace the original sphere by an oblate spheroid with the same volume. We then replace this spheroid with a disk of the same capacitance. We herein demonstrate this two-stage replacement uniquely defines the geometric parameters of the equivalent disks as well as the surface fraction occupied by the disks in the mean plane, which are used as input parameters for the trapping rate of a lattice of absorbing disks. Parameter I for a lattice of spheres is now approximated by the following expression:

$$I_{\text{sph}} = \frac{(1-\sigma/\sigma_c)^2}{(1+q_1\sqrt{\sigma}-q_2\sigma^2)}, \tag{18}$$

where σ is the surface fraction of the equivalent absorbing disks, and q_1, q_2 are lattice-type dependent parameters obtained from curve fitting using numerical data, as described in Ref. [51]. Parameter values for q_1 and q_2 for typical lattice arrangements are listed in Table I. Parameter σ_c is related to the maximum filling fraction of the lattice of disks.

Preservation of volume between the original sphere of radius a and the equivalent oblate spheroid of semimajor axis b and semiminor axis h gives $a^3 = hb^2$. Similarly, equivalence of capacitance yields $(b/h)^{1/3}(2/\pi) = 1$, which is a direct consequence of Eqs. (30) and (31) of Ref. [44] for $b \gg h$. These relations lead to the realization $b = (\pi/2)a$ and $h = (2/\pi)^2 a$, so that $h/b = (2/\pi)^3 \sim 0.26$, which is less than unity as required for an oblate spheroid. Subsequently, the surface fraction reduces to $\sigma = \pi b^2/S = (\pi^3/4)a^2/S$ where S is the area of the unit cell of the lattice as defined previously (noting that S is different for different lattice morphologies). The functional form of Eq. (18) is an interpolation of two asymptotic expressions that can be derived analytically from first principles. Specifically, $I \propto (1-\sigma/\sigma_c)^2$ when $\sigma \simeq 1$, and $(1-I) \propto \sqrt{\sigma}$ as $\sigma \to 0$. According to arguments presented in Ref. [51], a simplified assumption $\sigma_c \simeq 1$ can be used if σ is not too close to unity, and we also adopt this simplification in our study.

For the case of any lattice type, the following expression for parameter I separates the effect of lattice morphology and scatterer shape:

$$I = \frac{C_{0,\text{sph}}}{C_{0,\text{void}}} I_{\text{sph}}, \tag{19}$$

where $C_{0,\text{sph}} = 4\pi a$ as before and $C_{0,\text{void}}$ is the capacitance of a single void of arbitrary shape in open space. It is assumed here that the lattice dependence for the void of arbitrary shape is the same as for the spherical void.

Equation (19) has been derived for the bubble approximation limit given by $\mu \ll (3/4)B$. However, when the stiffness of the void interface is dominated by the shear modulus of the soft matrix, the scaling relation $\omega_0^2 \propto C_{0,\text{void}}$ may be significantly affected, whereby the resonance frequency of some arbitrary-shaped voids may be lower than that of a spherical void of the same volume. This finding has been previously reported in Refs. [16,36,53]. The resonance frequency of the void in free space is given by $\omega_0 = \sqrt{k/m}$, where m is the effective mass of the pulsating void and k is the stiffness of the void interface. For the effective mass, we have the same universal estimate as for the case of a bubble, $m = \rho/C_{0,\text{void}}$ [45]. Estimation of the interface stiffness is specific to the particular void shape. For a sphere, $k = \mu/\pi a^3$ where a is the radius of the sphere. For a disk-shaped void, $k = 3\mu/4a^3$ where a is now the radius of the disk [16,54]. Scaling for the interface stiffness can be achieved without imposing the condition of volume preservation of an equivalent sphere. Here the surface area of a void denoted by S_{void} is an appropriate candidate for the shape characterization. For $k \propto \mu/S_{\text{void}}^{3/2}$ and $m = \rho/C_{0,\text{void}}$ we arrive at the following scaling for the resonance frequency:

$$\omega_0 \propto c_t \sqrt{\frac{C_{0,\text{void}}}{S_{\text{void}}^{3/2}}}. \tag{20}$$

Substituting ω_0 into Eq. (2) and using the geometric scaling given by $C_{0,\text{void}} = \gamma_{\text{void}}\sqrt{S_{\text{void}}}$, where the coefficient γ_{void} is known for many basic shapes and has very weak shape dependency [55], we again recover Eq. (10) with parameter I as follows:

$$I \simeq \left(\frac{\gamma_{\text{sph}}}{\gamma_{\text{void}}}\right)^3 \left(\frac{C_{0,\text{void}}}{C_{0,\text{sph}}}\right)^2 I_{\text{sph}}. \tag{21}$$

III. RESULTS AND DISCUSSION

The effect of multiple scattering of longitudinal waves on the resonance frequency of a lattice of voids in a soft medium is herein investigated using our analytical model and compared with results obtained numerically as well as experimental data from Ref. [20]. This effect is initially examined for a square lattice of spherical voids, in terms of the ratio of void radius to lattice constant ranging from the maximum lattice constant ($a/d = 0$) to the full blockage limit ($a/d \to 0.5$). Figure 2 presents the monopole resonance frequency for a grating of voids normalized by the resonance frequency of a single spherical void in a soft medium of infinite extent. The analytical results were calculated using Eq. (6) and the two expressions for parameter I given by Eqs. (7) and (18), whereby the corresponding values of parameter I are shown in Fig. 3. For sparse configurations with very low values of a/d, predictions from the two expressions for parameter I are reasonably close, i.e., $I_{\text{sph}} \to 1$ and $\Omega \to \omega_0$ as $d \to \infty$. As $a/d \to 0$, Eq. (18) for a square lattice reduces to $I \simeq 1 - q_1\sqrt{\sigma} = 1 - 2.75\sqrt{\pi}(a/d)$. As a/d increases, I decreases and Ω/ω_0 increases, as a direct consequence of acoustic coupling between voids. Both expressions for parameter I

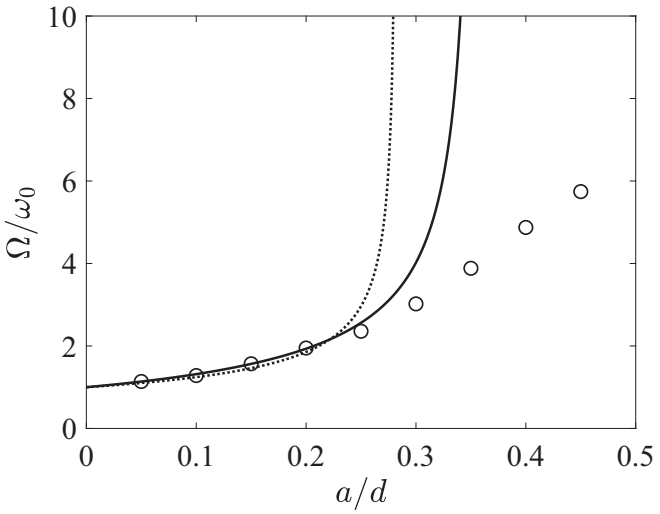

FIG. 2. Ratio of the monopole resonance frequency of a square lattice of spherical voids to the resonance frequency of a single spherical void in a soft elastic medium obtained analytically using Eqs. (6) and (7) (dotted line), Eqs. (6) and (18) (solid line), and numerically (circles).

predict that for some threshold value of a/d at which $I = 0$, $\Omega \to \infty$ corresponding to the disappearance of the system resonance. This threshold occurs at $a/d = 1/2\sqrt{\pi} \simeq 0.28$ for Eq. (7). Similarly, for the square lattice of spherical voids, this threshold occurs at $a/d = 2/\pi^{3/2} \simeq 0.36$ for Eq. (18) as $S = d^2$ and $\sigma = (\pi^3/4)(a/d)^2$. Our numerical model was developed using COMSOL Multiphysics (v5.4), in which we calculated the transmitted pressure for an array of voids in a soft medium. Monopole resonance frequency of the array of voids corresponds to the frequency of minimum sound transmission, as described in Ref. [21]. Good agreement between results obtained analytically and numerically can be observed at lower filling fraction, with results obtained analytically becoming invalid beyond a threshold value of a/d.

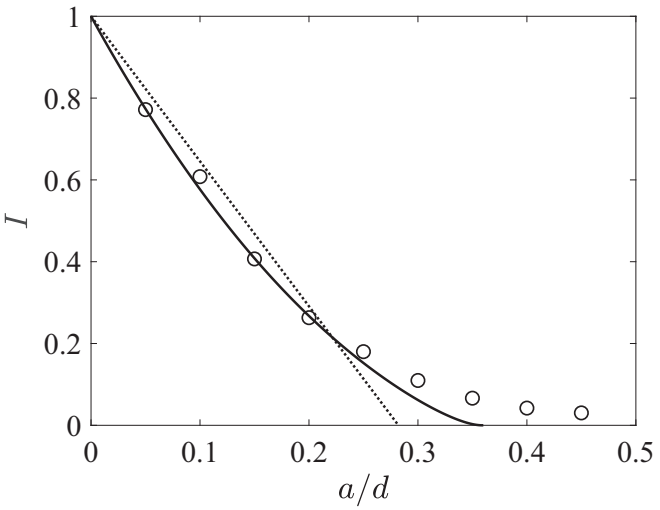

FIG. 3. Parameter I for a square lattice of spherical voids obtained analytically using Eq. (7) (dotted line), Eq. (18) (solid line), and numerically (circles).

TABLE II. Material and geometric properties of the phononic crystal.

Geometric properties	
Void radius	38.5 μm
Lattice constant in x direction	360 μm
Lattice constant in y, z directions	200 or 300 μm
Layers of voids in x direction	1 or 4
Material properties of rubber	
Density	1000 kg/m^3
Shear modulus	$1.6(1+i)$ MPa
Phase velocity	1.02 mm/μs
Attenuation	$3.2 \times 10^{-12}\omega^{1.45}$ mm^{-1}

As the next step in the validation of the proposed analytical framework, we compare the transmission coefficient obtained analytically with experimental data from Ref. [20]. The transmission coefficient for each void layer was calculated as $1 + r$, where r is the reflection coefficient given by Eq. (17). We used the geometric and material properties of the phononic crystal from Ref. [20], which are listed in Table II. Figures 4 and 5 present the transmission coefficient for two different values of lattice constant, for both a single layer and four layers of spherical voids using parameter I given by Eq. (18). In general, good agreement between results obtained analytically and experimentally can be observed. Small discrepancies at higher frequencies are attributed to normalization in the experimental results to remove the bulk attenuation through the crystal. For both a single layer and four layers of voids, high attenuation of sound over a broad frequency range occurs, attributed to monopole resonance. Comparison of Figs. 4 and 5 reveals greater sound attenuation is achieved for the lower value of lattice constant, associated with higher filling fraction of voids and greater resonance coupling.

We now present the effect of multiple scattering of waves for different lattice morphology and scatterer shape. Figure 6 compares parameter I for an array of spherical voids in square and triangular lattices, obtained analytically using Eq. (18) as well as numerically. Identical spacing between voids for both these lattice arrangements was used. For low a/d values, parameter I for spherical voids in square and triangular lattices is similar. At higher a/d values, parameter I for spherical voids in a triangular lattice is smaller compared to the corresponding square lattice, in agreement with our numerical simulations. Figure 7 compares parameter I for an array of spherical voids in a square lattice calculated using Eq. (18) with results obtained using Eq. (21) for an array of prolate spheroidal voids of aspect ratio 3 as well as an array of oblate spheroidal voids of aspect ratio 3, also in a square lattice. The semimajor and semiminor axes of the prolate spheroid with the same volume as a sphere of radius a are $2.08a$ and $a/1.44$, respectively. Similarly, the semimajor and semiminor axes of the oblate spheroid with the same volume as a sphere of radius a are $1.44a$ and $a/2.08$, respectively. The free-space capacitance of each spheroid was obtained from Ref. [45]. The ratio $\gamma_{\text{void}}/\gamma_{\text{sph}}$ for each spheroid was obtained from data of

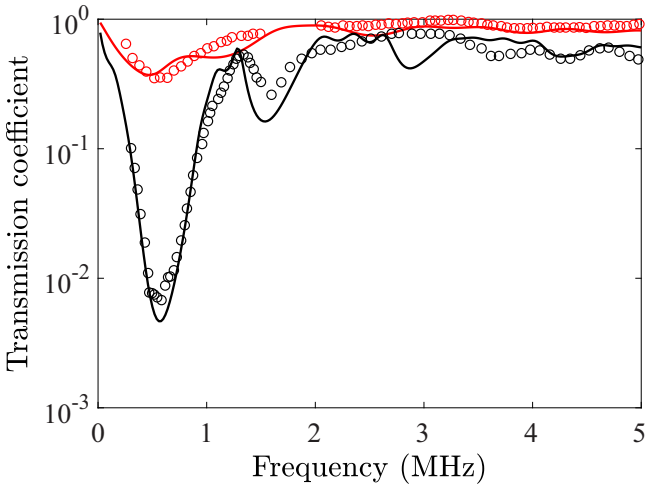

FIG. 4. Transmission coefficient of a single layer (red) or four layers (black) of spherical voids of radius $a = 38.5\,\mu$m in a square lattice with spacing $d = 300\,\mu$m embedded in a soft matrix obtained analytically using Eq. (18) (lines). Analytical results are compared with experimental results (circles) from Ref. [20].

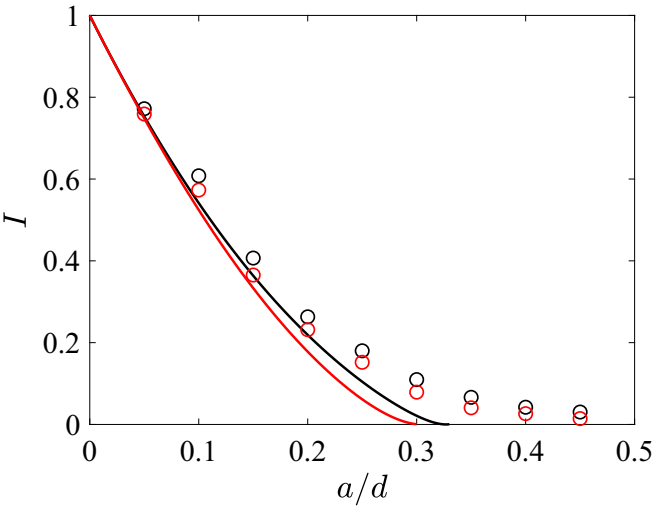

FIG. 6. Parameter I for spherical voids in a square lattice (black) and a triangular lattice (red) obtained analytically using Eq. (18) (solid lines) and numerically (circles).

Ref. [55], whereby the ratio for prolate and oblate spheroids of aspect ratio 3 corresponds to $\gamma_{\text{void}}/\gamma_{\text{sph}} = 1.023$ and 0.986, respectively. The monopole resonance for an array of spheroidal voids was obtained numerically as the frequency of minimum sound transmission and converted to I using the monopole resonance of a single spheroidal void from Ref. [45]. The discrepancy between the analytical and numerical results for spheroidal voids at low a/d values arises from differences in the scaling relation for a spherical void given by $\omega_0^2 \propto C_{0,\text{void}}$ and for voids of complex shape given by Eq. (20), whereby the latter is approximately derived using dimensional analysis. Table III compares parameter I as $a/d \to 0$ for the scatterers of different shape and lattice type. Comparison of Figs. 6 and 7 highlights that for the same shaped void in different lattice arrangements (Fig. 6), values of parameter I are similar for low a/d and diverge as a/d increases. Further, it has been verified that parameter I for spherical voids in different lattices is almost identical when plotted as a function of $a/\sqrt{S}$ (results not shown), in agreement with results reported in Ref. [31]. In contrast, for differently shaped voids in the same lattice arrangement (Fig. 7), values for parameter I differ at low a/d but converge to the same value as a/d increases.

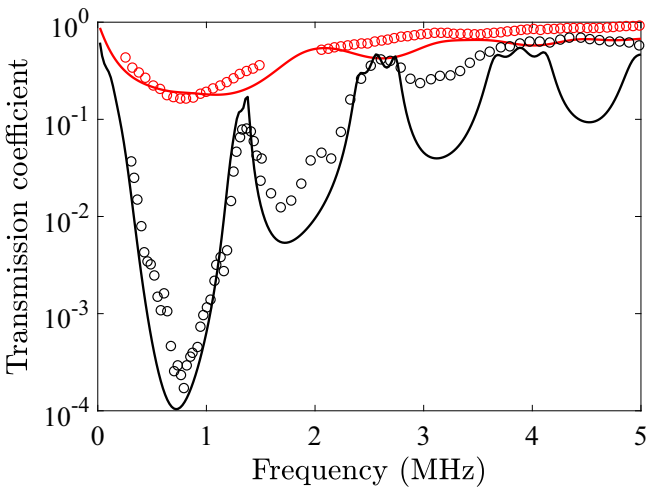

FIG. 5. Transmission coefficient of a single layer (red) or four layers (black) of spherical voids of radius $a = 38.5\,\mu$m in a square lattice with spacing $d = 200\,\mu$m embedded in a soft matrix obtained analytically using Eq. (18) (lines). Analytical results are compared with experimental results (circles) from Ref. [20].

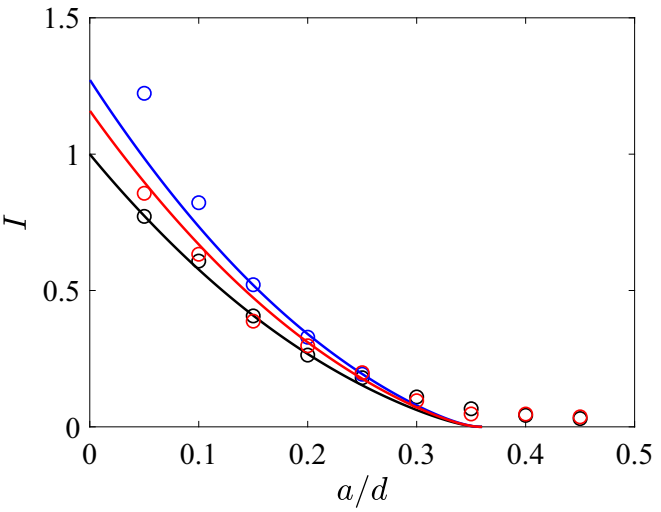

FIG. 7. Parameter I for spherical voids in a square lattice obtained analytically using Eq. (18) (black line), prolate spheroidal voids (red line), and oblate spheroidal voids (blue line) of aspect ratio 3 in a square lattice obtained analytically using Eq. (21). Analytical results are compared with numerical results (circles).

TABLE III. Parameter I for different lattice type and scatterer shape as $a/d \to 0$.

Equation number	Void shape	Lattice type	Parameter I
(18)	Spherical	Square	$1 - 2.75\sqrt{\pi}(a/d)$
(18)	Spherical	Triangular	$1 - 2.73\sqrt{\pi}(a/d)$
(21)	Prolate spheroidal	Square	$1.16 - 3.19\sqrt{\pi}(a/d)$
(21)	Oblate spheroidal	Square	$1.27 - 3.49\sqrt{\pi}(a/d)$

IV. CONCLUSIONS

We have derived an analytical framework for interaction of acoustic waves with a periodic lattice of resonant voided scatterers in a soft elastic material. Our framework employs an effective boundary condition for the lattice of the scatterers and an analogy with electrostatics. Our expression for the reflection coefficient is generalized to include voids of arbitrary shape and different lattice morphology. Further, our method is not restricted to maintain the same configuration of scatterers at each layer of the crystal (including shape of the individual scatterer and lattice type). The proposed model can be further generalized by including clustering arrangements of scatterers, since expressions for effective capacitance are available for many of these cases. Due to the exact solution describing acoustic wave propagation using the transfer matrix method, the proposed model provides a simple yet consistent approach for simulation of the multiple scattering phenomena in any layered configuration of voided scatterers, provided multiple scattering effects are incorporated in the expression for the reflection coefficient. We believe that the approach introduced here can provide important insights for exploring new wave phenomena, acoustic tomography, and targeted material design.

[1] M. R. Haberman and A. N. Norris, Acoust. Today **12**, 31 (2016).
[2] A. A. Maznev and V. E. Gusev, Phys. Rev. B **92**, 115422 (2015).
[3] F. Luppé, J.-M. Conoir, and A. N. Norris, J. Acoust. Soc. Am. **131**, 1113 (2012).
[4] J. Zhu, Y. Chen, X. Zhu, F. J. Garcia-Vidal, X. Yin, W. Zhang, and X. Zhang, Sci. Rep. **3**, 1728 (2013).
[5] A. N. Norris, Proc. R. Soc. London A **464**, 2411 (2008).
[6] D. Bigoni, S. Guenneau, A. B. Movchan, and M. Brun, Phys. Rev. B **87**, 174303 (2013).
[7] M. Lanoy, J. H. Page, G. Lerosey, F. Lemoult, A. Tourin, and V. Leroy, Phys. Rev. B **96**, 220201(R) (2017).
[8] S. Guenneau, A. Movchan, G. Pétursson, and S. A. Ramakrishna, New J. Phys. **9**, 399 (2007).
[9] S. M. Ivansson, J. Acoust. Soc. Am. **119**, 3558 (2006).
[10] E. Ruffino and P. Delsanto, J. Acoust. Soc. Am. **108**, 1941 (2000).
[11] O. Lombard, C. Barrière, and V. Leroy, Europhys. Lett. **112**, 24002 (2015).
[12] R. V. Craster and S. Guenneau, *Acoustic Metamaterials: Negative Refraction, Imaging, Lensing and Cloaking* (Springer Science & Business Media, New York, 2012).
[13] J. Zhu, J. Christensen, J. Jung, L. Martin-Moreno, X. Yin, L. Fok, X. Zhang, and F. Garcia-Vidal, Nat. Phys. **7**, 52 (2011).
[14] Y. A. Ilinskii, E. A. Zabolotskaya, and M. F. Hamilton, in *AIP Conf. Proc.* (AIP, New York, 2012), Vol. 1474 pp. 255–258.
[15] H. Zhao, J. Wen, D. Yu, and X. Wen, J. Appl. Phys. **107**, 023519 (2010).
[16] D. C. Calvo, A. L. Thangawng, C. N. Layman Jr, R. Casalini, and S. F. Othman, J. Acoust. Soc. Am. **138**, 2537 (2015).
[17] V. Leroy, A. Strybulevych, M. Lanoy, F. Lemoult, A. Tourin, and J. H. Page, Phys. Rev. B **91**, 020301(R) (2015).
[18] T. Brunet, J. Leng, and O. Mondain-Monval, Science **342**, 323 (2013).
[19] J. Li and C. T. Chan, Phys. Rev. E **70**, 055602(R) (2004).
[20] V. Leroy, A. Bretagne, M. Fink, H. Willaime, P. Tabeling, and A. Tourin, Appl. Phys. Lett. **95**, 171904 (2009).
[21] G. S. Sharma, A. Skvortsov, I. MacGillivray, and N. Kessissoglou, Wave Motion **70**, 101 (2017).
[22] G. S. Sharma, A. Skvortsov, I. MacGillivray, and N. Kessissoglou, J. Acoust. Soc. Am. **141**, 4694 (2017).
[23] J. Zhong, H. Zhao, H. Yang, J. Yin, and J. Wen, Appl. Acoust. **145**, 104 (2019).
[24] Y.-F. Wang, Y.-S. Wang, and X.-X. Su, J. Appl. Phys. **110**, 113520 (2011).
[25] Y.-F. Wang and Y.-S. Wang, J. Sound Vib. **332**, 2019 (2013).
[26] T. Valier-Brasiera, J.-M. Conoir, F. Coulouvrat, and J.-L. Thomas, J. Acoust. Soc. Am. **138**, 2598 (2015).
[27] G. S. Sharma, A. Skvortsov, I. MacGillivray, and N. Kessissoglou, J. Sound Vib. **443**, 652 (2019).
[28] P. A. Martin, *Multiple Scattering: Interaction of Time-Harmonic Waves with N Obstacles* (Cambridge University Press, Cambridge, 2006).
[29] L. L. Foldy, Phys. Rev. **67**, 107 (1945).
[30] Z. Ye, Acta Acust. united Ac. **89**, 435 (2003).
[31] V. Leroy, A. Strybulevych, M. Scanlon, and J. Page, Eur. Phys. J. E **29**, 123 (2009).
[32] B. Liang and J.-C. Cheng, Phys. Rev. E **75**, 016605 (2007).
[33] D. V. Sivukhin, Sov. Phys. Acoust. **1**, 82 (1955).
[34] E. Meyer, K. Brendel, and K. Tamm, J. Acoust. Soc. Am. **30**, 1116 (1958).
[35] L. D. Landau and E. M. Lifshitz, *Theory of Elasticity* (Pergamon Press, London, 1970).
[36] D. C. Calvo, A. L. Thangawng, and C. N. Layman, J. Acoust. Soc. Am. **132**, EL1 (2012).
[37] Y. A. Kobelev, Acoust. Phys. **61**, 392 (2015).
[38] Y. A. Kobelev, Acoust. Phys. **57**, 749 (2011).
[39] Y. A. Kobelev, Acoust. Phys. **60**, 1 (2014).
[40] A. Bretagne, A. Tourin, and V. Leroy, Appl. Phys. Lett. **99**, 221906 (2011).
[41] L. Brekhovskikh, *Waves in Layered Media* (Academic Press, London, 1980).
[42] M. L. Munjal, *Acoustics of Ducts and Mufflers with Application to Exhaust and Ventilation System Design* (John Wiley & Sons, Toronto, 1987).
[43] M. Strasberg, J. Acoust. Soc. Am. **25**, 536 (1953).

[44] K. S. Spratt, K. M. Lee, P. S. Wilson, and M. S. Wochner, in *Proc. Meetings on Acoustics 166 ASA* (ASA, San Francisco, 2013), Vol. 20, p. 045004.
[45] K. S. Spratt, M. F. Hamilton, K. M. Lee, and P. S. Wilson, J. Acoust. Soc. Am. **142**, 160 (2017).
[46] N. Kanev and M. Mironov, Acoust. Phys. **51**, 89 (2005).
[47] L. Schwan, O. Umnova, and C. Boutin, Wave Motion **72**, 154 (2017).
[48] J.-J. Marigo and A. Maurel, J. Acoust. Soc. Am. **140**, 260 (2016).
[49] V. Leroy, N. Chastrette, M. Thieury, O. Lombard, and A. Tourin, Fluids **3**, 95 (2018).
[50] P. L. Krapivsky, S. Redner, and E. Ben-Naim, *A Kinetic View of Statistical Physics* (Cambridge University Press, Cambridge, 2010).
[51] A. M. Berezhkovskii, M. I. Monine, C. B. Muratov, and S. Y. Shvartsman, J. Chem. Phys. **124**, 036103 (2006).
[52] C. B. Muratov and S. Y. Shvartsman, Multiscale Model. Simul. **7**, 44 (2008).
[53] S. M. Ivansson, J. Acoust. Soc. Am. **124**, 1974 (2008).
[54] M. Rahman, Philos. Mag. A **79**, 1923 (1999).
[55] Y. Chow and M. Yovanovich, J. Appl. Phys. **53**, 8470 (1982).